Journal of Ionic Liquids 5 (2025) 100178

Contents lists available at ScienceDirect

Journal of Ionic Liquids

journal homepage: www.elsevier.com/locate/jil

Spinning of wheat straw-based pulp into cellulosic multifilaments by 1-Ethyl-3-methylimidazolium octanoate as direct solvent

Antje Ota [*,a], Marc P. Vocht [a], Ronald Beyer [a], André van Zomeren [b], Ilona van Zandvoort [b], Jaap W. van Hal [b], Frank Hermanutz [a]

[a] German Institutes of Textile and Fiber Research Denkendorf (DITF), Koerschtalstr. 26, D-73770 Denkendorf, Germany
[b] Netherlands Organization for Applied Scientific Research (TNO), Westerduinweg 3, 1755 LE Petten, , Netherlands

ARTICLE INFO

Keywords:
Cellulose
Ionic liquid
Man-made cellulosic fibers
Filament
Dry-jet wet spinning
Wheat straw

ABSTRACT

The demand for man-made cellulosic fibers is rapidly increasing; however, these fibers are mainly based on wood dissolving pulp. Faster growing crops, such as agricultural residues and annual fast-growing plants (i.e. hemp), are attractive alternative raw materials as well.e report on the use of wheat straw pulp (WS) for the spinning of continuous man-made cellulosic fibers based on an ionic liquid spinning technology. Filaments were produced from bleached and unbleached WS pulp that were obtained by an acetone based organosolv fractionation Commercial dissolving pulp based on hardwood (HW) was used as reference pulp Continuous filaments were spun using a novel dry-jet wet spinning (HighPerCell® process) technique, which is based on the use of 1-ethyl-3-methylimidazolium octanoate ([C_2C_1im] [Oc]) as a solvent. Via this approach, continuous multifilament filaments were spun in textile and technical quality filament yarns. Elongation at break up to 9 % and tenacities of 35 cN/tex were obtained for the WS filaments. The novel approach also allows the preparation of low wet fibrillating cellulosic filaments appropriate for textile applications. It should be emphasized that only recycled IL was used in the production of the filaments and sustainable pulping technology.

1. Introduction

Cotton currently has the largest market share of natural cellulose-based textile fibers. Forecasts assume that total global annual textile fiber production increases from 113 million tons in 2021 to 133.5 million tons by 2030, while cotton production is expected to remain static between 26 and 28 million tons annually (Haemmerle, 2011). The resulting "cellulose gap" must be closed by increasing fiber production from wood-based pulp and through the utilization of additional cellulosic sources, such as annual plants, waste streams, and recycled cotton-rich fabrics (El Seoud et al., 2020). The production of dissolving pulp is currently depending on wood, while trees take a long time to grow but the forest is also straggling due to the climate crisis and the replacement of plastics due to national bioeconomy strategy. Cellulose from faster-growing annual plants can also be extracted and used to spin man-made cellulosic fibers (MMCFs) and, therefore, offer opportunities to close the cellulose gap. MMCFs production was revived in several reviews, and the different processes were compared (Sayyed et al., 2019). The Viscose and Lyocell spinning technologies are currently available at industrial scale. Overall, the Viscose process is the major MMCF-spinning technology. The Lyocell process, which is based on a direct solvent, is less commonly used (Rosenau et al., 2002; Bredereck and Hermanutz, 2005). Viscose requires alkaline ageing of the pulp before spinning and is associated with the use of toxic CS_2 and 650–850 kg water per 1 kg of viscose fibers. Extensive waste treatment has become cost determining for this process. The Lyocell process does not require pretreatment of the pulp but uses a cyclic amine (N-Methylmorpholine N-oxide) as a solvent. This makes the process much more efficient and environmentally friendly.

Pulps from annual crops such as hemp, flax and wheat straw or rice straw offer a more rapid increase in pulp volume due to the higher growth rate of the plants (Paulitz et al., 2017; Makarov et al., 2022; Urdaneta et al., 2024). Fast-growing crops are considered to have a high potential for carbon sequestration, though agriculture is a major emitter of greenhouse gases (mainly nitrous oxide) (Conchedda and Tubiello, 2020; Seile et al., 2022; McDonald et al., 2021). Especially fast-growing annual plants with a high cellulose and alpha cellulose – cellulose of high purity – are considered an alternative to wood pulp. Ateş et al.

* Corresponding author.
E-mail address: antje.ota@ditf.de (A. Ota).

https://doi.org/10.1016/j.jil.2025.100178
Received 13 August 2025; Received in revised form 10 October 2025; Accepted 10 October 2025
Available online 11 October 2025

compared the chemical compositions of different agricultural residues (Ateş et al., 2015). Due to the high alpha cellulose content (> 65 %) and low lignin content, hemp pulp is of main interest for fiber production, which was described by different research groups (Paulitz et al., 2017; Thümmler et al., 2022). Recently, hemp pulp was tested into continuous filament spinning process using ionic liquids as direct solvent. It could be successfully shown that alternative pulp are applicable as alternative feedstock in novel spinning techniques (Ota et al., 2023). Although, annual plant pulps have a high potential to become next generation the pulping processes still need to be adapted for different plant types (Vera et al., 2023). Lignocellulosic biomass such as wheat straw or rice straw usually have high ash contents, in particular silica as main component. Silica is a structural element in the cell wall of plants and is therefore not easily removed from the biomass. In general, wheat straw consists of cellulose (33–55 %), hemicellulose (18–35 %), lignin (7–30 %), and small quantities of other components, such as protein, wax and inorganic compounds as well as up to 14 % inorganic components (Li et al., 2019). Effective and high-value-added utilization of agricultural straw is still challenging. Currently, only a fraction has been converted into low-value products (feedstuff, soil fertilizer and paper). The use of wheat straw pulp for textile application using common spinning techniques is quite challenging. In particular residual metal ions or inorganic impurities (silica, potassium, calcium) after the pulping process can have a negative effect on filtration and spinning stability as well as fiber properties. The Lyocell process, where *N*-Methylmorpholine *N*-oxide (NMMO) is used as solvent, requires a much more complex purification process for wheat straw compared to wood pulp (Rosenau et al., 2002). The pressure on closing the cellulose gap and increasing the share of MMCF for textile market is so high that finding new solvents for cellulose spinning became of main interest for many research groups. In 2002 the Group around R. D. Rogers published the first paper in which they described the solubility of cellulose in an ionic liquid (IL) (Swatloski et al., 2002). Like NMMO, some ionic liquids (ILs) can be used as direct solvents for cellulose, and so for fiber spinning. This was reviewed by different researchers (Hermanutz et al., 2018; Azimi et al., 2022; Szabó et al., 2023). If the physico-chemical properties are carefully selected, ILs can be a safer spinning solvent than NMMO. Furthermore, the percentage of dissolved cellulose can be substantially higher. In addition, a solvent recycling rate above 99.9 % can be reached, ending up with an economical feasible process and comparable with lyocell. At early research stages, 1-ethyl-3-methyl imidazolium acetate and 1-ethyl-3--methyl imidazolium diethyl phosphate were the first IL that have been evaluated for fiber spinning of cellulose within our group. (Olsson and Westman, 2013) In the last 10 years we focused on the usage of octanoate as anion, namely 1-ethyl-3-methylimidazolium octanoate [C_2C_2im] [Oc]) as a solvent for filament spinning (HighPerCell® technology) (Vocht et al., 2021). In comparison to [C_2C_2im] [Ac] we observed higher stretching rates during spinning which minimizes the fiber diameter and allows the production of supermicro fibers for instance. In addition, a higher thermal stability was proven for [C_2C_2im] [Oc] which is an advantage in recyclability of the ionic liquid due to less degradation. This work is a proof of concept of the production of high-quality cellulosic filaments from wheat straw using the patented FABIOLA™ process for the pulp production and HighPerCell® for filament spinning (Smit and Huijgen, 2017).

2. Experimental

2.1. Materials

Upgraded unbleached (UB) and bleached (B) wheat straw-pulps (WS) produced by Netherlands organization for applied scientific research (TNO) were used for filament spinning. Virgin

1-ethyl-3-methylimidazolium octanoate ([C_2C_1im] [Oc]) was supplied in technical grade by Proionic (AT). Based on the knowledge that no influence on fiber spinning and properties are expected by re-use of the solvent, the spinning trails were performed with recycled ionic liquids (see supporting information Figure S1).

2.2. Pulp preparation (Fabiola^{TM})

Wheat straw (WS) pre-extraction and subsequent fractionation was done using the Fabiola® process at Fraunhofer following the procedure described in Smit et al. (Smit et al., 2022). Pulp upgrading was performed to remove (silicon) ash content using previously optimized process conditions. The selected process conditions (0.5 M NaOH, 4 h, 80 °C) were applied with 1 kg pulp in an autoclave (Kiloclave Büchi Glas Uster AG, Switzerland) equipped with a 20 L vessel. Part of the upgraded pulp (WS-UB) was subsequently bleached with sodium chlorite following the procedure described by Smit and Huijgen (Smit and Huijgen, 2017). All details can be found in supplementary information (SI).

2.3. Pulp characterization

The ash content was determined gravimetrically after heating the samples to 575 °C and maintaining the temperature for 6 h according to DIN 54,370. Determination of the metal ion content was conducted according to DIN EN ISO 11,885 using the ICP-OES instrument ICAP 7400 (Thermo Fisher Scientific). Alkali resistance (R-18 value) was determination using an 18 wt % sodium hydroxide solution according to DIN 54 355. Size exclusion chromatography (SEC) was performed using a Shimadzu Nexera LC-40D, operated at 80 °C, combined with a Shimadzu RI-detector, operated at 60 °C. A PLgel mixed-B pre-column and PLgel mixed-B separation column (linear separation range: 500–10,000,000 g/mol) were used. DMAc/LiCl (9 g/L) was used as a solvent (flow rate 0.75 mL/min). A conventional calibration versus Pullulan standards (PSS Mainz, Mn = 342–1330,000 g/mol) was applied. Detailed sample preparation was previously described (Vocht et al., 2021). Mass average molar mass (M_W), number average molar mass (M_n), and dispersity (Đ) were calculated. Additionally, the degree of polymerization (*DP*) was evaluated according to DIN 54,270.

2.4. Filament spinning and fiber characterization

Electron beam (EB) irradiation was performed for reducing pulps *DP* in a controlled manner, with an EC-LAB 400 electron beam device from Electron Crosslinking AB. All pulp plates (thickness of 0.5–1 mm) were irradiated on both sides applying 40 kGy (in total 80 kGy) and an acceleration voltage of 180 keV. This was performed at room temperature and atmospheric pressure. Dope preparation was done in a two-stage procedure starting with mixing pulp and the IL at room temperature for 30 min. To obtain a homogenous spinning solution the mixture was continuously processed via a thin film evaporator (VTA GmbH & Co. KG) applying a rotational frequency of 100 Hz at 60 mbar and 120 °C. The spinning dope was then filled into a pressure filtration cauldron (Karl-Kurt Juchheim Laborgeräte GmbH). All dopes had a concentration of 12 wt %. Rheological properties of the dopes were measured using a rheometer (MCR 301, Anton Paar) with parallel-plate geometry (25 mm plate diameter, 1 mm gap). Dynamic moduli (storage modulus *G*' and loss modulus *G*'') and the complex viscosity (η^*) were determined by performing dynamic oscillatory experiments between 110 and 20 °C applying shear rates (between 0.1 and 100 s^{-1}) and a deformation of 10%. Zero-shear viscosity (η_0) was calculated by fitting the Carreau Gahleitner model (Gahleitner and Sobczak, 1989). Multi-filaments were spun on a laboratory-scale device (Dienes Apparatebau GmbH) at spinning temperatures of 65 and 75 °C respectively. The spinning dope was passed through a metallic filter (mesh size of 0.043 mm). The extruder was heated and propelled the spinning dope through a multi-hole spinneret (250 capillaries, 450 μm capillary length, 150 μm capillary diameter) into a 1-meter coagulation bath containing water at 18 °C via an air gap (10 mm) at an injection speed of 1.5 m/min.

Filaments were wound on godets at velocities between 8.5 and 17.0 m/min before running through two washing baths, each one meter in length, and two washing godets. Before being wound onto a bobbin, the fibers were tempered (80 °C) on a heated godet, see Figure S1. We previously proved that there are no major changes in the fiber properties if the IL concentration in the coagulation bath rises during spinning (Vocht et al., 2021). This finding opens the possibility to operate the spinning at a relatively high concentration of the IL (up to 20 wt %) in the coagulation bath and potentially reduces the energy costs during solvent recovery.

Scanning electron microscopy (SEM) was carried out on a field emission scanning electron microscope (*Zeiss*, type Auriga) with an acceleration voltage of 3 keV. An Inlens-SE-detector was used for fracture surfaces and a secondary electron detector for fiber surfaces, respectively. Cellulosic fiber samples were sputtered with Pt/Pd (SEM, layer thickness ca. 5 nm) for preparation. The total orientation of the cellulosic fibers was determined by birefringence (Δn) measurements using a Leitz Laborlux 12POL polarization microscope ($\lambda = 546$ nm) equipped with a Leitz compensator B. Fiber samples were cut wedge-shaped and wetted with paraffin oil. Δn was obtained by dividing the measured retardation of the polarized light (Γ) by the respective fiber diameter (d). The total orientation (f_t) was obtained by dividing Δn by the maximum birefringence of cellulose ($\Delta n_{max} = 0.062$) (Lenz et al., 1992). It was assumed that the maximum birefringence values of the amorphous and crystalline phase are identical, i.e. $\Delta n_{cr}(max) = \Delta n_{am}(max) = 0.062$ (Lenz et al., 1992; Lenz et al., 1993).

$$\Delta n = \frac{\Gamma}{d}$$

$$f_t = \frac{\Delta n}{\Delta n_{max}}$$

For Wide-angle X-ray scattering (WAXS), a Rigaku D/Max Rapid II was used at 40 kV and 30 mA with Cu Kα radiation ($\lambda = 1.54059$ Å). A shine monochromator and an image plate detector were used. The scanning rate was 0.2°/min and the scanning step 0.1° All fibers were aligned in a fiber sample holder.

The degree of crystallinity (C.I.) was calculated according to the peak deconvolution method using pseudo-Voigt functions (Seo et al., 2013). Integrated intensities of the crystalline (I_c) and the amorphous reflections (I_a) were determined.

$$C.I. = \frac{\sum I_c}{\sum I_c + I_a}$$

The crystallite chain orientation was determined by an azimuthal scan of the meridional main interference taken from well-aligned fiber samples in the longitudinal direction. The degree of preferred relative orientation of the [002] crystallites (P.O.) was calculated according to the following equation:

$$P.O. = \frac{180^\circ - FWHM\ [002]}{180^\circ}$$

Wet fibrillation tests were evaluated by fixing single filaments (2.5 cm length) to a frame and placing them in a cylinder containing 20 mL of distilled H_2O and 9 g of zirconia spheres (0.75–1 mm). Testing was performed in a Labomat at 30 °C for 3 h and a rate of 50 rpm. Depending on the counted fibrils, fibrillation was classified between 1 and 6 (Table 1).

Table 1
Wet fibrillation index (fb_i) of the tendency to fibrillate.

Counted fibrils	fb_i
0–5	1
6–10	2
11–20	3
21–40	4
41–80	5
> 80	6

Mechanical fiber properties of single filaments were measured on a Textechno Favimat+ (20 °C, 60 % humidity) to obtain an average result from 20 different single filaments according DIN ISO 5079 and for testing under wet conditions DIN ISO 53 816. Fineness was measured as weight in grams per 10,000 m of filament (dtex in the textile industry). Boiling shrinkage was determined according DIN EN 14,621. Filaments were placed for 15 min in boiling water and their shrinkage was determined. Sweat test was done with 3 cycles in alkaline and acidic sweat, the fibres were dried at 37 °C afterwards.

3. Results and discussion

3.1. Pulp composition

The determined R-18 values of the different pulps were comparable and ranged from 90 to 95 %. R-18 (alpha cellulose) value describes the amount of the cellulose material, which is not dissolved in an 18 % NaOH solution and is commonly used to describe the pulp quality (Hermanutz et al., 2018; Zhang et al., 2018; Fechter et al., 2020). While the commercial HW pulp possessed an R18 value of 90 %, cellulose contents of respectively 94 % and 95 % were measured for the WS pulps, unbleached (WS-UB) and bleached (WS-B), (Table 2). All pulps had initial *DP*s over 900, Table 1. Such high *DP*s lead to highly viscous solutions where either an increased spinning temperature is needed for spinning or lower cellulose concentration has to be chosen, which also disfavored due to demand of energy or lower efficiency, respectively. Usually, the *DP* must be reduced to a value lower than 800. There are different ways to shorten the cellulose chains and increase the dope concentration (Hwang et al., 2020). In previous papers we showed that electron beam radiation (EB), a non-chemical method, is a suitable process to adjust the DP of pulps (Ota et al., 2023; Vocht et al., 2021). This process is based on the splitting of the cellulose chains, increase the available surface area and reduces the crystallinity (Driscoll et al., 2009; Seo et al., 2013). The latter two are beneficial for the dope preparation using [C_2C_1im] [Oc] (Ota et al., 2023). Irradiation of the pulps was executed by applying an EB dose of 80 kGy, resulting in DPs between 650 and 410 and a dispersity index ($Đ$)of 6 - 8 for all pulps, Fig. 3 and Table 2. It can be also seen that the molecular weights (M_n) were very similar after EB treatment for all pulps. Establishing a precise correlation between DP and SEC data is challenging, because DP is a direct measure while SEC is an indirect measurement technique. Defining this quantitative relationship is an important research topic that should be the focus of a separate, dedicated study. As the DP is also commonly used by industrial spinning of cellulose we have designated using DP as the governing parameter for evaluating the spinnability of cellulosic feedstocks. SEC measurements are primarily done to understand the

Table 2
DP, R 18 value, Mn, Mw, $Đ$ and ash content of the cellulose pulp before and after EB irradiation.

Pulp		EB dose/ kGy	DP_{FeTNa}	M_n[1]/ kg/mol	M_W[2]/ kg/mol	$Đ$[3]	R 18/ %
HW	before EB	0	930	35	435	13	90
	after EB	80	650	33	311	8	
WS-UB	before EB	0	1320	37	646	17	94
	after EB	80	410	35	295	8	
WS-B	before EB	0	1160	81	1204	15	95
	after EB	80	440	37	230	6	

[1] Number average molecular weight; [2]weight average molecular weight; [3]dispersity index.

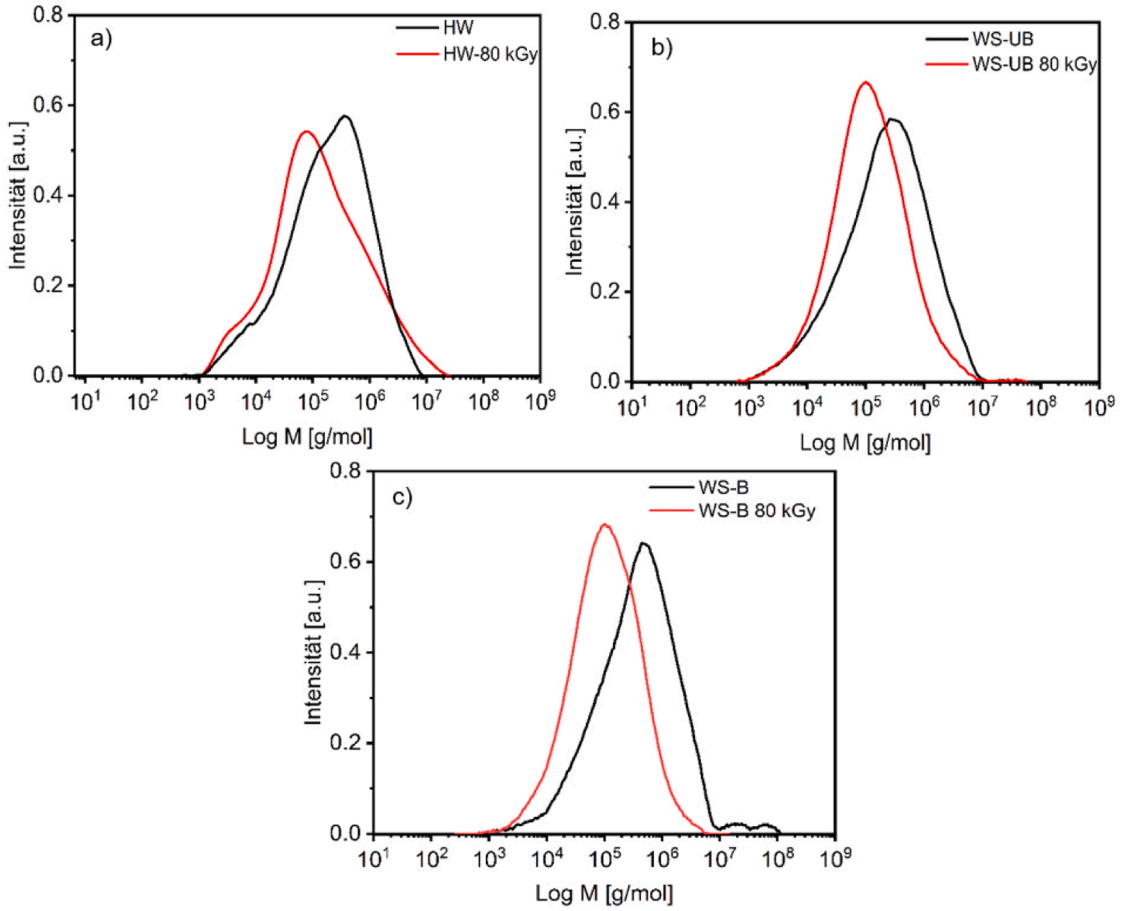

Fig. 3. Molecular weight distribution diagrams before (black) and after irradiated with 80 kGy (red) of the pulps a) HW, b) WS-UB, and c) WS-B.

EB-degradation process better

Small amounts of ash were found (below <0.5 wt %) in all pulps (Table 3). The lowest amount of heavy metal content and silicon were found for the industrial wood pulp (HW). Nevertheless, the bleached (WS-B) and unbleached (WS-UB) samples showed low amounts of silicon as well. Via bleaching of the WS pulp the total amount of ash could be significantly reduced by 77 % to 0.11 %. It was noted that all metal ion values are acceptable and within the tolerance level and no known negative effect for [C_2C_1im] [Oc]-based spinning processes is expected. In contrast to the Viscose or Lyocell process, where transition metal ions interfere with the processes, e.g. these ions can react with NMMO during the Lyocell process, resulting in exothermic reactions (Rosenau et al., 2002).

Table 3
Ash content and ICP-OES analysis of the pulps.

Pulp		HW	WS-UB	WS-B
Ash content / wt %		0.06	0.48	0.11
Metal ion / ppm	**Fe_{total}**	4	67	53
	Cu^{2+}	<1.0	26	<1.0
	Ni^{2+}	<2.0	<2.0	<2.0
	Mn_{total}	<2.0	<2.0	<2.0
	Cr_{total}	<1.0	21	7
	Si	33	300	110
	S	76	85	61
	Na / K	220 / <4	290 /16	170 / 74
	Mg / Ca	17 / 73	18 / 300	3 / 27

3.2. Rheology and fiber spinning

The rheology profiles of the cellulose/IL dopes were used to determine their spinnability and the conditions to perform the spinning trail (Olsson and Westman, 2013; Ingildeev et al., 2013). For viscoelastic spinning dopes, a crossover point ($G' = G''$) is expected at a specific frequency (ω_S). Spinning solutions consisting of 12 wt % cellulose in [C_2C_1im] [Oc] displayed non-Newtonian viscous behavior. As a result, a shear-thinning behavior of the viscoelastic fluid was observed, Fig. 4. With decreasing temperature, the ω_S decreased while zero-shear viscosity (η_0) increased, a typical behavior for polymeric solutions. All solutions showed a suitable η_0 range, which is essential for spinnability and typically between 1000 −10.000 Pa ·s.

Based on the rheology measurements, 75 °C (HW) and 65 °C (WS) were chosen the for spinning trials. The multifilament bundles produced were extruded into a coagulation bath (water) after passing an air gap of 10 mm and continuously washed with water. Table 4 summarizes the parameters for fiber spinning based on the air gap (dry-jet wet) spinning process. For all spinning trials, no clogging of the nozzle was observed, and continuous filaments were spun without any failures. The spinning trials confirmed an important operational tolerance: the water coagulation bath remained stable even at elevated IL concentrations. The stability is highly valuable, as the ability to operate with a higher solvent concentration in the bath means less water must be distilled during the solvent recovery cycle. Draw ratios (DRs) were varied from 3 to 27 in order to modify the filament properties. Low DRs yielded in higher elongation filaments (textile quality), while increasing the DR led to higher tenacity filaments (technical quality). Highly stretched yarns are mainly used as reinforcement fibers due to higher strength while yarn with higher elongation at break are preferred for apparel. Obtained

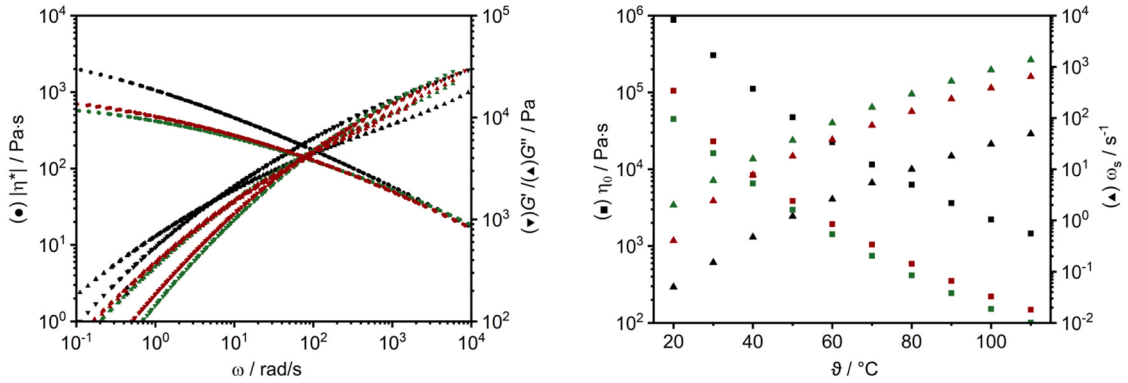

Fig. 4. Rheological behavior of the spinning dope (12 wt % cellulose HW (black), WS-UB (red). and WS-B (green) in [C_2C_1im] [Oc]) left: master curve at reference temperature 70 °C, |η*| (●), *G'* (▾), *G''* (▲); right: rheological parameters η_0 (■) and ω_S (▲) in dependence of temperature.

Table 4
Air gap spinning conditions of 12 wt % [C_2C_1im] [Oc] spinning solution.

Spinning trial	Temperature/ °C	η_0 / Pa•s	ω_S/ s^{-1}	max. DR
HW	75	8889	8	11
WS-UB	65	1484	55	20
WS-B	65	1084	121	27

filaments on bobbins are shown in Fig. 5.

3.2.1. *Characterization of the filaments*

The obtained filaments, had an average linear density between 1.9 and 2.8 dtex (diameter between 9 μm and 16 μm), which is typical for man-made cellulosic fibers. Note that 1 dtex is the linear density defined as Grams per 10,000 m of yarn.

Because of the rapid coagulation of cellulose, all fibers showed a smooth surface with no visible defects. The round cross section of the fibers (Fig. 6, right side) is a result of the dry-jet wet spinning technique. Due to the preorientation of the molecular chains in the air gap all fibers showed a fibrillar structure network (Ingildeev et al., 2013). The fibers did not show any visible voids or signs of a skin-core structure in the cross-section, representative SEM images are shown in Fig. 6. As reported in a previous publication there were no residual amounts of IL residue present in the HighPerCell® filaments (Vocht et al., 2021).

For all three pulps the spinning conditions were varied to achieve textile and technical filament quality, see Table 5 and Table 6. For a better comparison of the fibers we picked similar DRs, respectively 4 and 11 for textile and technical fiber quality. The shrinkage during drying was 3.0 % and 0.25 %, respectively. The mechanical tensile properties of the single filaments were measured under dry and wet conditions according to DIN norm. Though, spinning HW pulp higher tensile strengths (33–40 cN/tex) and Young's moduli (1800–2200 cN/tex) were observed under dry conditions. Technical fiber showed compared values to lyocell fibers (35–40 cN/tex), where textile quality is also the range of viscose fibers that possess fibers strength between 20–25 cN/tex. WS filaments had tenacities between 18–28 cN/tex and Young's moduli between 1000–1800 cN/tex. This difference might be due to the lower molecular weight (M_n) of the HW pulp as described by other researchers (A. Michud et al., 2015). No major differences in the mechanical filament properties from bleached and unbleached WS pulps were observed, reflecting the tailorable character of this IL-based process to different pulp origins. Apparently, there is no influence of the impurities originating from the raw material in case of the wheat straw, even lower ash content in the bleached pulp did not increase the tenacity or elongation values for both technical and textile fiber quality. Therefore, it is more dependent on the molecular structure of the cellulose. Due to shorter cellulose chains of WS (DP) less covalent bonding between the cellulose chains is possible and lower strength is observed. All filament types also showed the typical behavior when testing the mechanical properties under wet conditions with an increase of the elongation at break values and decreased tenacity and Young's modulus.

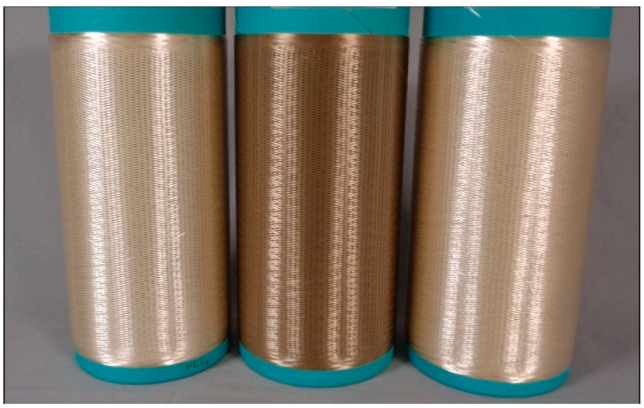

Fig. 5. Filaments left (HW), middle (WS-UB) and right (WS-B).

Depending on the spinning conditions, the microfibril chain orientation differs. A high chain orientation along the longitudinal fiber axis (P.O. values) and total orientation (f_t) leads to the delamination of the fiber; this phenomenon is called fibrillation. Fibrillating fibers will show a "peach skin-like" appearance and affects textile processes (weaving, dyeing and finishing) (Bates et al., 2006; Ma et al., 2016). Fibrillation occurs under wet mechanical abrasion and results in disintegration of the fibers. In case of HW and WS filaments it can be nicely correlate with the spinning conditions (DR and shrinkage) applied to result in two fiber qualities, namely textile and technical. To maintain the quality of textiles during wearing and washing, fibrillation has to be minimized. Table 5 shows the comparison between the total orientation (f_t) – measured via birefringence – and the wet fibrillation index (fb_i) – mechanical stability under wet conditions. In general, higher orientated filaments showed a higher fibrillation tendency. This effect is also related to the draw ratio as higher ratios result in most cases in higher tenacity. A reverse trend was seen for filaments with a lower total orientation /lower DRs. To describe this filament-type the term "textile" is used. Additional like the f_t the diffraction, patterns correlated with the fibrillation and, hence, the spinning conditions. "Textile" filaments showed a typical semi-crystallinity cellulose II kind patterns with a higher share of an amorphous part (crystallinity index between 60 and 74) while "technical" filaments showed sharper crystalline reflexes (crystallinity index between 76 and 78), Figure S3 and Figure S4. The "technical" filaments showed higher tenacity, while the lower elongation at break for this filament type is also directly correlated with the fiber structure (Vocht et al., 2021; Zhu et al., 2016). The textile quality

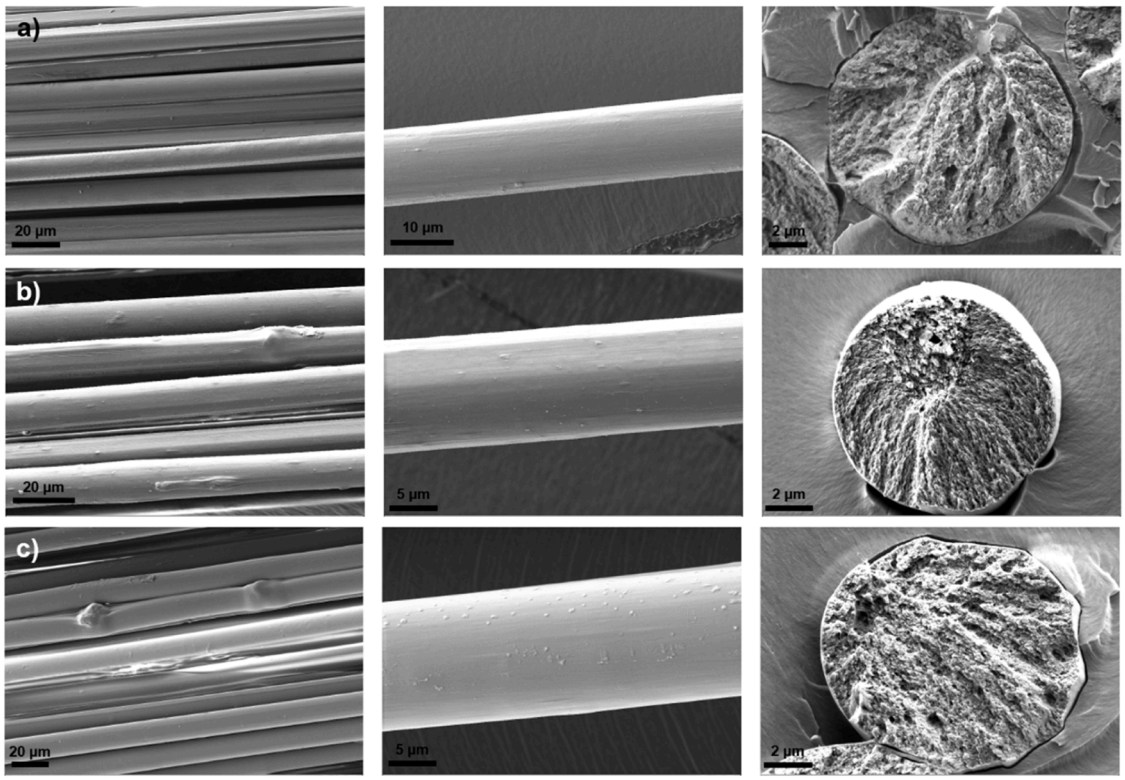

Fig. 6. SEM images of the fibers a) HW, b) WS-UB and c) WS-B.

Table 5
Mechanical (dry and wet) mean value of 20 measurements, total orientation (f_t), crystallinity index (*C.I.*), preferred orientation (P.O.) and fibrillation index (fb_i), mean value of 3 measurements, of "textile" filaments.

	HW		WS-UB		WS-B	
Draw Ratio	**4**		**4**		**4**	
Shrinkage / %	**3.0**		**3.0**		**3.0**	
Testing conditions	**dry**	**wet**	**dry**	**wet**	**dry**	**wet**
Titer / dtex	1.94 ± 0.05	2.11 ± 0.05	2.32 ± 0.24	1.96 ± 0.12	2.34 ± 0.15	2.42 ± 0.20
Elongation at break / %	10 ± 1	14 ± 1	9 ± 1	16 ± 2	8 ± 1	15 ± 3
Tensile strength / cN/tex	33 ± 1	18 ± 1	20 ± 2	12 ± 2	18 ± 2	10 ± 1
Young's modulus / cN/tex	1798 ± 51	112 ± 8	1075 ± 43	61 ± 4	1044 ± 45	50 ± 4
f_t	0.63 ± 0.02		0.54 ± 0.01		0.53 ± 0.02	
***C.I.* / %**	74		60		74	
***P.O.* [002]**	88		85		86	
fb_i	2		2		2	

Table 6
Mechanical (dry and wet), mean value of 20 measurements total orientation (f_t), crystallinity index (*C.I.*), preferred orientation (P.O.) and fibrillation index (fb_i), mean value of 3 measurements, of "technical" filaments.

	HW		WS-UB		WS-B	
Draw Ratio	**12**		**11**		**11**	
Shrinkage / %	**0.25**		**0.25**		**0.25**	
Testing conditions	**dry**	**wet**	**dry**	**wet**	**dry**	**wet**
Titer / dtex	1.75 ± 0.11	1.80 ± 0.11	2.02 ± 0.10	1.96 ± 0.12	2.30 ± 0.08	2.28 ± 0.13
Elongation at break / %	8 ± 1	8 ± 1	4 ± 1	7 ± 1	4 ± 1	8 ± 1
Tenacity / cN/tex	40 ± 2	23 ± 1	27 ± 2	14 ± 1	28 ± 3	12 ± 1
Young's modulus/ cN/tex	2225 ± 95	314 ± 14	1835 ± 41	226 ± 11	1777 ± 66	163 ± 13
f_t	0.70 ± 0.03		0.64 ± 0.02		0.66 ± 0.01	
***C.I.* / %**	78		76		78	
***P.O.* [002]**	92		91		90	
fb_i	5		4		5	

filaments show only few fibrils on the surface while many fibrils are visible in case of the technical quality, Fig. 7. Filaments with low and high fibrillation can be produced using the IL-technology (HighPerCell® process) by simply varying the process conditions without the need of chemicals or time-consuming post-spinning treatment (Ingildeev et al., 2013; A. Michud et al., 2015), surpassing the Lyocell fibers, as a treatment (cross-linking) is essential for specific applications.

The stability of the spinning dope and whether ageing occurs was evaluated by spinning the same dope over 16 days. This was tested using WS-UB and the same spinning conditions were chosen in terms of spinneret configuration, spinning speed, temperature (80 °C) and draw ratio to observe any differences in the filament properties, Fig. 8 and Table S2. For all fibers the elongation at break remained mostly constant over time in comparison to the starting values of ~4 % and a tenacity of ~ 35 cN/tex. Here the effect of the spinning temperature also has to be emphasized, increasing the spinning temperature led to an increased tenacity (35 cN/tex) and Young's modulus (around 2000 cN/tex) compared to the technical WS-UB fibers spun at 65 °C (27 cN/tex and 1800 cN/tex). Both findings show the stability and the flexibility of the dope and the process.

Another important quality control test for fibers is the so-called boiling shrinkage test, which is used to specify the dimensional stability of textiles, for example after washing. The boiling shrinkage test showed a lower shrinkage for the textile filaments compared to technical filament, Fig. 9.

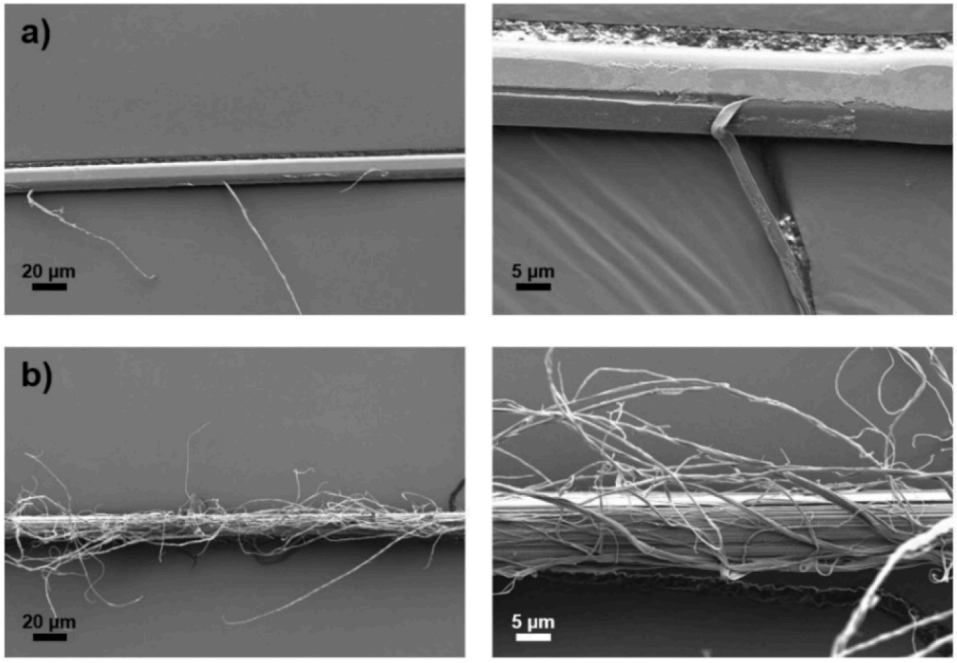

Fig. 7. SEM images of WS-UB filaments after wet fibrillation testing a) textile quality and b) technical quality.

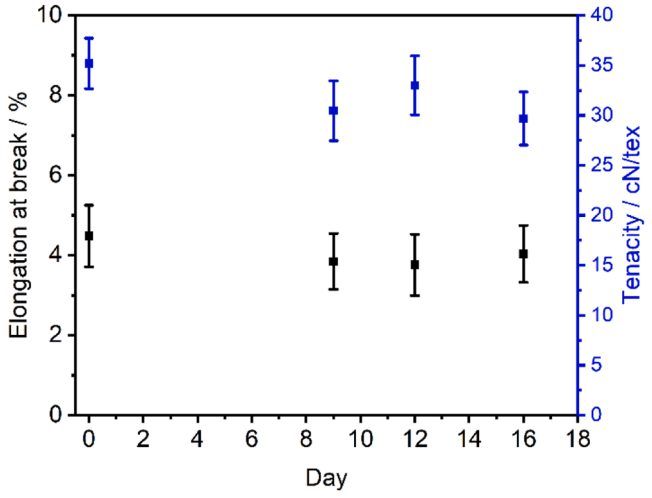

Fig. 8. Mechanical properties (elongation at break (black) and tenacity (blue)) of the filaments of the WS-UB dope ageing test.

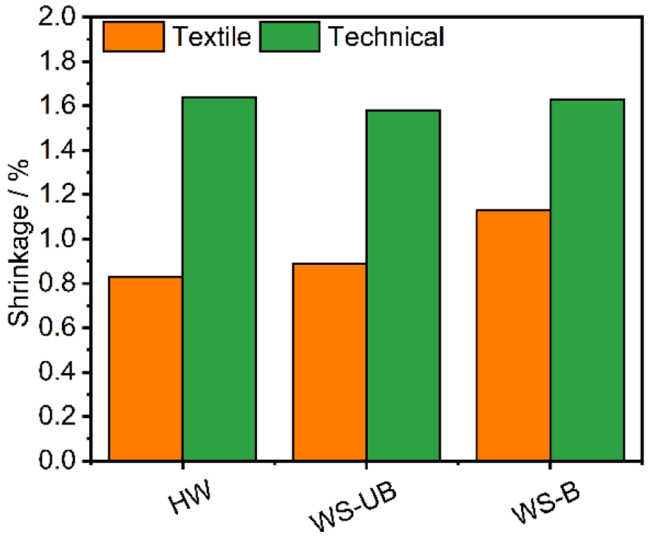

Fig. 9. Shrinkage of textile (orange) and technical (green) filaments from HW, WS-UB and WS-B.

There was no significant change of the mechanical properties after the boiling shrinking test (Table S3 S.I.), except for the Young's modulus of all technical filaments where a loss around 30 % was observed regardless of the pulp origin (Fig. 10). This drop was also observed in case of the textile HW filaments. This difference could be caused by the relaxation (softening of non-crystalline regions within the cellulose microfibrils, relaxation of oriented amorphous regions or crystallite slippage) of the fibers during the boiling shrinkage test. No analytics were performed. Therefore, no evidence or comprehensive conclusion is possible.

4. Conclusions

This study focused on analyzing the potential filament production using HighPerCell® technology and wheat straw pulp produced via an acetone-based organosolv process. HW dissolving pulp was used as a reference material. The unbleached and bleached WS pulps had high cellulose purity and were suitable for IL-based dope preparation. Filament dry-jet wet spinning was successfully performed with the different pulps. WS-based filaments showed slightly lower mechanical properties compared to HW pulp filaments due to a different molecular structure of the cellulose. Nonetheless, the influence of the spinning conditions (DR, shrinkage) and the resulting fiber structure nicely revealed the flexibility of the spinning technology without using any chemical for determining structural properties. Furthermore, it should be emphasized that a local available feedstock was processed using sustainable, energy- and resource-efficient biorefinery and spinning technologies with recycled solvent use. This is essential for the transition to a sustainable and circular textile value chain. Future work should expand the focus beyond hemp and wheat straw to include other annual plants. We aim to investigate the influence of the different molecular structures of cellulose—specifically, those derived from wood versus non-wood

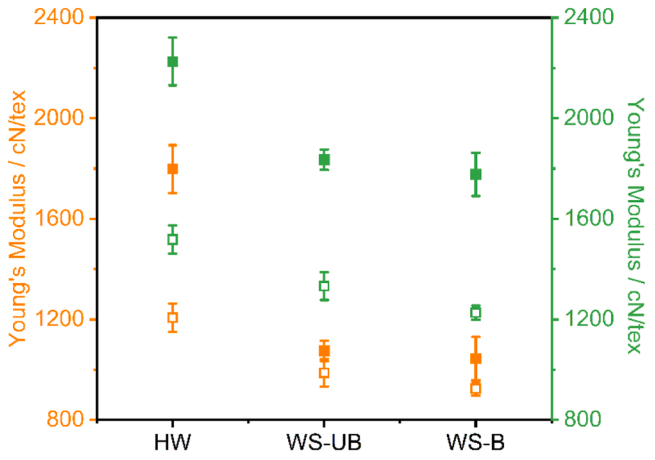

Fig. 10. Young's modulus of HW, WS-UB and WS-B of textile (orange) and technical (green) filaments before (closed symbols) and after (open symbols) boiling shrinkage test.

sources—to better understand their impact on filament properties. These basic studies will help develop models for local supply chains of raw materials usable with the HighPerCell® technology (i.e., "drop-in" solutions depending on seasonal availability of feedstock). Furthermore, pulp production methods are of interest, as they significantly influence pulp composition and reactivity. Finally, as the textile industry moves toward circularity, fiber-to-fiber recycling is an important subject for further study.

CRediT authorship contribution statement

Antje Ota: Writing – review & editing, Supervision, Project administration. **Marc P. Vocht:** Writing – original draft, Visualization, Investigation. **Ronald Beyer:** Investigation, Formal analysis. **André van Zomeren:** Writing – review & editing, Project administration. **Ilona van Zandvoort:** Writing – review & editing, Investigation. **Jaap W. van Hal:** Funding acquisition, Conceptualization. **Frank Hermanutz:** Writing – review & editing, Supervision, Funding acquisition.

Declaration of competing interest

The authors declare that they have no known competing financial interests or personal relationships that could have appeared to influence the work reported in this paper.

Acknowledgements

This work is part of the project HEREWEAR and has received funding from the European Union's Horizon 2020 research and innovation program under grant agreement No 101000632. Sabine Henzler, Ulrich Hageroth, Alexandra Mueller, Esther Cobussen-Pool, Michiel Hoek, Petra Bonouvrie, Ben van Egmond, Peter Rensen and Karina Vogelpoel-de Wit, are kindly acknowledged for their contributions to the experimental work and analyses.

Supplementary materials

Supplementary material associated with this article can be found, in the online version, at doi:10.1016/j.jil.2025.100178.

Data availability

The authors do not have permission to share data.

References

Ateş, S., DenİZ, İ., Kirci, H., AtİK, C., Okan, O.T., 2015. Turk. J. Agric. For 39, 144–153. https://doi.org/10.3906/tar-1403-41.
Azimi, B., Maleki, H., Gigante, V., Bagherzadeh, R., Mezzetta, A., Milazzo, M., Guazzelli, L., Cinelli, P., Lazzeri, A., Danti, S., 2022. Cellulose 29, 3079–3129. https://doi.org/10.1007/s10570-022-04473-1.
Bates, I., Maudru, E., Phillips, D.A.S., Renfrew, A.H.M., Su, Y., Xu, J., 2006. Color. Technol. 120, 293–300. https://doi.org/10.1111/j.1478-4408.2004.tb00233.x.
Bredereck, K., Hermanutz, F., 2005. Rev. Prog. Color. Relat. Top. 35, 59–75. https://doi.org/10.1111/j.1478-4408.2005.tb00160.x.
Conchedda, G.; Tubiello, F.N., Emissions due to agriculture. Global, regional and country trends 2000–2018. Environmental team, F. S. D., FAOSTAT *Analytical Brief Series*, Ed. Rome, 2020; Vol. 18.
Driscoll, M., Stipanovic, A., Winter, W., Cheng, K., Manning, M., Spiese, J., Galloway, R. A., Cleland, M.R., 2009. Radiat. Phys. Chem. 78, 539–542. https://doi.org/10.1016/j.radphyschem.2009.03.080.
El Seoud, O.A., Kostag, M., Jedvert, K., Malek, N.I., 2020. Macromol. Mater. Eng., 1900832 https://doi.org/10.1002/mame.201900832.
Fechter, C., Fischer, S., Reimann, F., Brelid, H., Heinze, T., 2020. Cellulose 27, 7227–7241. https://doi.org/10.1007/s10570-020-03151-4.
Gahleitner, M., Sobczak, R., 1989. Kunst.-Ger. Plast. 79, 1213–1216.
Haemmerle, F.M., 2011. Lenzinger Ber 89, 12–21.
Hermanutz, F., Vocht, M.P., Panzier, N., Buchmeiser, M.R., 2018. Macromol. Mater. Eng., 1800450 https://doi.org/10.1002/mame.201800450.
Hwang, Y., Park, H.-J., Potthast, A., Jeong, M.-J., 2020. Cellulose. https://doi.org/10.1007/s10570-020-03604-w.
Ingildeev, D., Effenberger, F., Bredereck, K., Hermanutz, F., 2013. J. Appl. Polym. Sci. 128, 4141–4150. https://doi.org/10.1002/app.38470.
Lenz, J., Schurz, J., Wrentschur, E., 1992. Acta Polym 43, 307–312. https://doi.org/10.1002/actp.1992.010430603.
Lenz, J., Schurz, J., Wrentschur, E., 1993. Colloid Polym. Sci. 271, 460–468. https://doi.org/10.1007/BF00657390.
Li, J., Zhang, X., Zhang, J., Mi, Q., Jia, F., Wu, J., Yu, J., Zhang, J., 2019. Carbohydr. Polym. 223, 115057. https://doi.org/10.1016/j.carbpol.2019.115057.
Ma, Y., Hummel, M., Määttänen, M., Särkilahti, A., Harlin, A., Sixta, H., 2016. Green Chem. 18, 858–866. https://doi.org/10.1039/c5gc01679g.
Makarov, I.S., Golova, L.K., Smyslov, A.G., Vinogradov, M.I., Palchikova, E.E., Legkov, S. A., 2022. Fibers 10. https://doi.org/10.3390/fib10050045.
McDonald, H., Frelih-Larsen, A., Lóránt, A., Duin, L., Pyndt Andersen, S., Costa, G., Bradley, H., 2021. Carbon farming, Making agriculture Fit For 2030. European Union, Luxemburg. https://doi.org/10.2861/099822. Environment, P. H. a. F. S. E. c.
Michud, A., Hummel, M., Sixta, H., 2015a. Polymer (Guildf) 75, 1–9. https://doi.org/10.1016/j.polymer.2015.08.017.
Michud, A., Tanttu, M., Asaadi, S., Ma, Y., Netti, E., Kääriainen, P., Persson, A., Berntsson, A., Hummel, M., Sixta, H., 2015b. Text. Res. J. 86, 543–552. https://doi.org/10.1177/0040517515591774.
Olsson, C., Westman, G., 2013. J. App. Polym. Sci. 127, 4542–4548. https://doi.org/10.1002/app.38064.
Ota, A., Vocht, M.P., Beyer, R., Reboux, A., Reboux, C., Hermanutz, F., 2023. Fibers 11. https://doi.org/10.3390/fib11110090.
Paulitz, J., Sigmund, I., Kosan, B., Meister, F., 2017. Procedia Eng. 200, 260–268. https://doi.org/10.1016/j.proeng.2017.07.037.
Rosenau, T., Potthast, A., Adorjan, I., Hofinger, A., Sixta, H., Firgo, H., Kosma, P., 2002. Cellulose 9, 283–291. https://doi.org/10.1023/A:1021127423041.
Sayyed, A.J., Deshmukh, N.A., Pinjari, D.V., 2019. Cellulose 26, 2913–2940. https://doi.org/10.1007/s10570-019-02318-y.
Seile, A., Spurina, E., Sinka, M., 2022. Fibers 10. https://doi.org/10.3390/fib10090079.
Seo, Y.B., Lee, M.W., Park, D.H., Park, H.J., 2013. Ind. Eng. Chem. Res. 52, 692–695. https://doi.org/10.1021/ie300521w.
Smit, A., Huijgen, W., 2017. Green Chem. 19, 5505–5514. https://doi.org/10.1039/C7GC02379K.
Smit, A.T., Verges, M., Schulze, P., van Zomeren, A., Lorenz, H., 2022. ACS Sustain. Chem. Eng. 10, 10503–10513. https://doi.org/10.1021/acssuschemeng.2c01425.
Swatloski, R.P., Spear, S.K., Holbrey, J.D., Rogers, R.D., 2002. J. Am. Chem. Soc. 124, 4974–4975. https://doi.org/10.1021/ja025790m.
Szabó, L., Milotskyi, R., Sharma, G., Takahashi, K., 2023. Green Chem. 25, 5338–5389. https://doi.org/10.1039/D2GC04730F.
Thümmler, Katrin, Fischer, Johanna, Fischer, Steffen, Kosan, Birgit, Meister, F., 2022. Lenzinger Ber. 97, 25–31.
Urdaneta, F., Kumar, R., Marquez, R., Vera, R.E., Franco, J., Urdaneta, I., Saloni, D., Venditti, R.A., Pawlak, J.J., Jameel, H., Gonzalez, R.W., 2024. Ind. Crop. Prod. 221. https://doi.org/10.1016/j.indcrop.2024.119379.
Vera, R.E., Vivas, K.A., Urdaneta, F., Franco, J., Sun, R., Forfora, N., Frazier, R., Gongora, S., Saloni, D., Fenn, L., Zhu, J.Y., Chang, H.-m., Jameel, H., Gonzalez, R., 2023. J. Clean. Prod. 429. https://doi.org/10.1016/j.jclepro.2023.139394.
Vocht, M.P., Beyer, R., Thomasic, P., Müller, A., Ota, A., Hermanutz, F., Buchmeiser, M. R., 2021. Cellulose 28, 3055–3067. https://doi.org/10.1007/s10570-021-03697-x.
Zhang, S., Chen, C., Duan, C., Hu, H., Li, H., Li, J., Liu, Y., Ma, X., Stavik, J., Ni, Y., 2018. Bioresources 13, 1–16. https://doi.org/10.15376/biores.13.2.Zhang.
Zhu, C., Richardson, R.M., Potter, K.D., Koutsomitopoulou, A.F., van Duijneveldt, J.S., Vincent, S.R., Wanasekara, N.D., Eichhorn, S.J., Rahatekar, S.S., 2016. ACS Sustain. Chem. Eng. 4, 4545–4553. https://doi.org/10.1021/acssuschemeng.6b00555.